

# **An Experimental Investigation of the Impact of Retrofitting an Underwater Stern Foil on the Resistance and Motion**

**Hongbo Hou<sup>1</sup>, Mateusz Krajewski<sup>2</sup>, Y. Kaan Ilter<sup>3</sup>, Sandy Day<sup>1</sup>,  
Mehmet Atlar<sup>1</sup>, Weichao Shi<sup>1\*</sup>**

**1 Department of Naval Architecture, Ocean & Marine Engineering,  
University of Strathclyde, UK**

**2 Malin Group, South Rotunda, 100 Govan Road, Glasgow, G51  
1AY, UK**

**3 Istanbul Technical University**

**Corresponding Author:**

**Weichao Shi, [weichao.shi@strath.ac.uk](mailto:weichao.shi@strath.ac.uk)**

**Department of Naval Architecture, Ocean & Marine Engineering,**

**University of Strathclyde**

**Henry Dyer Building, 100 Montrose Street,**

**Glasgow G4 0LZ, U.K.**

**Tel: 0141 548 3237**

## **Abstract**

Due to growing concerns about the environment and increasing prices in fuel, Energy Saving Device are becoming more and more important for ship. Hull Vane is an Energy Saving Device that can be retrofitted to the existing vessels or designed to new builds. This paper investigates the effect of retrofit to reduce the ship resistance and to improve the motion response in still water and sea states based on experimental tests. After the Hull Vane with Rhodes St. Gense 32 profile is designed and applied on a model DTMB 5415 hull in 1:51 scale with different attack angles and locations, the various experiments are conducted in the Kelvin Hydrodynamics Laboratory, University of Strathclyde. The model test shows Hull Vane can reduce and smoothen the stern wake markedly and significantly reduce the total resistance of ship. Pitch and heave motion of ship can be reduced by Hull Vane, because of which the comfort and operability of ship can be improved.

Keywords Hull Vane, Energy Saving Device, Model tests, Resistance, Motion in waves

# 1 Introduction

## 1.1 Hull Vane and Energy Saving Devices

Due to the growing concerns about the environment impact caused by modern shipping, research effort has been devoted to searching for energy-saving devices to reduce fuel consumption and CO<sub>2</sub> emission of ships. Recently Hull Vane as an underwater fixed foil fitted after the stern of the vessel has also been introduced to the market as an Energy Saving Device (ESD), which states to have the ability to save energy by reducing resistance. It was invented by van Oossanen in 1992. After years of testing and optimization, it was successfully launched in 2014 with claims of reducing the fuel consumption by 29% (Andrew, 2015) .

Hull Vane has a similar look to the traditional hydrofoil, as shown in Fig. 1. And the principle to reduce total drag of Hull Vane and hydrofoil is different. The overall resistance reduction generated by the Hull Vane can be decomposed into four distinct effects:

- Creating forward lift in the longitudinal direction providing the additional thrust force;
- Vertical component of the lift is effectively correcting the trim by causing bow-down moment;
- Negative pressure on the top side of the foil is affecting and reducing the wave and stern wake generation;
- In the waves, the vane reduces the motion of the vessel and added wave resistance.

Together with Hull Vane, there are also other types of ESDs, which are generally based on two different principles, i.e. drag reduction or propulsion enhancement. Hull Vane together with Interceptors, Stern End Bulbs, and Bow foils represent 4 different design concepts but share some similarities.

Interceptors which is shown in Fig. 2 can control the trim so that to reduce the resistance of the vessel when the vessel is moving. Interceptor is a vertical plate usually fitted to the transom of the smaller vessels and protruding several centimeters

below the transom. Due to the sudden variation in the flow caused by a deployed interceptor, overpressure is generated. At the higher speeds, this effect results in a decrease in resistance of the vessel as the trim of the vessel can be controlled to the optimum (PENSA and DE LUCA, 2011). The reduction in fuel consumption can be as high as 10-15% (Day and Cooper, 2011). However, it can only be achieved at high speeds close to planning. At lower speeds ( $F_n < 0.4$ ) device will introduce a significant raise in parasitic drag. Efficient interceptor requires to be controlled at least in 3 parts by a dedicated control system (Avci et al., 2018). Although the interceptor was developed for small, fast vessels, in recent years Delatamarin and MARIN proposed to investigate the effect of the interceptor on the cruise ship hull. The use of the plate provided 2% further reduction in resistance in comparison to the vessel with stern flap (Allema, 2005).

Stern End Bulb is a bulbous shaped appendix fixed to the stern of the vessel, as shown in Fig. 3. The principle of this idea is similar to the principle of the bulbous bow, which recovers the energy from the generated waves in order to reduce total resistance (Karafiath, 2012). It is a very rare concept that is claiming the reduction in the resistance is in the region of 5-7% (Karafiath, 2012). Due to being at the concept stage, more tests are required to understand the impact of the shape of the bulb and the impact between the bulb and the stern width. Due to the difference between the stern breadth and Stern End Bulb, the interaction between the flow and the Stern End bulb are not as significant as the interaction between the flow and bulbous bow. Thus, the final reduction in resistance is in much lower region.

Bow foils are streamlined hydrofoil fins connected to the bow area of the hull, as shown in Fig. 4. Foils can be fixed or pivoting depending on the vessel motion due to the waves. Its primary purpose is to contribute additional propulsion force by generating forward lift or by the push effect of the pivoting foil. The principle of this device is to create the 'pushing' power by the flapping foil. The thrust will be generated when the vertical lift force is synchronized with the heave velocity of the foil (Bowker et al., 2015). This technology has been used to aid propulsion of vessels in the past. More recently, It is used to be the main thruster in small unmanned vessels. Additionally, the device can contribute to damping the vessel motions, improving operability (Bøckmann, 2015). Researches show that bow foils can reduce fuel consumption by

up to 20% (Bøckmann and Steen, 2013). However, the device is not protected in case of the collision and has an increased chance of the damage in narrow and shallow passages as it is located below the keel.

From the listed four distinct effects of Hull vane to reduce resistance, it can be seen that Hull vane is the combination of the other three energy saving devices. It can reduce total resistance by reducing the stern wave generation, which is also the principle of Stern End Bulb to reduce total resistance; It can reduce total resistance by correcting the trim, which is also the principle of Interceptor to reduce resistance; and it can generate additional thrust, which is also the principle of bow foil. The relationship between these four energy saving devices is summarised in the Table 1.

## **1.2 Investigations about the Hull Vane**

From the researches, it can be seen that Hull vane can reduce more resistance than Stern End Bulb. Compared to Stern End Bulb, another advantage of operability of the vessel is that Hull vane can be a damping generator to reduce the vessel motion in wave, which can improve operability of the vessel. Compared to Interceptors, the researches show that the resistance reduction ability of Hull vane is slightly better than the ability of Interceptors. However, just like the comparison with Stern End Bulb, the advantage of Hull vane is that it can be a damping generator to improve operability of the vessel. The similarity between the Interceptors and the Hull vane is that both of them can only reduce total resistance when the velocity of vessel is high. The Interceptors will increase the resistance when the  $F_n$  is less than 0.4 (Avci et al., 2018) and the most effective region of Froude number for ship with hull Vane is between 0.2 and 0.7 (Andrew, 2015). Compared to Bow foils, the researches show that the resistance reduction ability of the two energy saving devices is very close. And both them can be a damping generator to improve the operability of the vessel, the advantage of Hull Vane is that it is not as easy as Bow foils to be damaged because of the installation position. Investigation around the Hull Vane

A number of studies about the Hull Vane show that it is an effective device to reduce ship resistance significantly. And Hull Vane is suitable for the vessels with relatively high displacement at a wider operating speeds range (Bouckaert, 2018).

The most effective region of Froude number for ship with hull Vane is between 0.2 and 0.7 (Andrew, 2015). Below this speed region, Hull Vane will introduce additional friction drag component. Beyond this speed region, the vertical lift component will create extremely high 'bow down' moment contributing to total resistance increase. The CFD simulations (Andrew, 2015) shows that the Hull Vane applied on 1.5-meter-long AMERCRC series model leads to 14.33%, 10.53% and 8.05% resistance reduction when Froude numbers are 0.5, 0.6 and 0.7 respectively.

Furthermore research based on CFD method for the Hull Vane on the DTMB 5415 destroyer was performed in 2016 (UITHOF K, 2016). This research has shown the resistance will decrease by 1.7%, 8.4% and 6.7% when the speed is 18, 24 and 30 knots respectively. This study also stated that application of the Hull Vane is relatively more suitable for modern and full after bodies.

Hull Vane is proved capable to reduce total resistance by 15.3% for 108m Holland-Clas OPV (Bouckaert et al., 2016). The CFD study has also analysed performance of the vessel in waves, it was observed that the application of the Hull Vane can reduce heaving RMS by 2.4%, pitching RMS by 8.1% and added resistance by 4.9% in the 2-meter-high waves. Another study (Uithof et al., 2016) based on CFD simulation shows that Hull Vane application on AMEREC 13 can significantly influence resistance and trim behaviour of the ship in waves. And resistance reduction of up to 32.4% is observed, the resistance reduction depends on the vertical and horizontal location of the Hull Vane. It is pointed out that longitudinal position of the vane has a great impact on the performance than the vertical.

In 2017, Suastika performed CFD simulation of the stern foil influence on ship resistance and performed towing tank test for validation of the simulation results. A model of 40m planning hull Orela was used for the study. He observed that the resistance coefficient,  $C_T$ , starts to decrease after keeping increasing and reaches the maximum value at 'resistance barrier' when the Froude number is in a low region. It was discovered that resistance increase can reach up to 13.9% when the Froude number is less than 0.45 and the resistance reduction of up to 10% can be observed when the Froude number is over 0.55, while the resistance barrier occurs when the Froude number is approximately 0.47 (Suastika et al., 2017).

Based on the above studies, Hull Vane has been explored as a retrofit or new built concept. However, it is still lack of a publically available study to comprehensive explore the design and optimisation of hull vane, experimental investigation of application on large vessels, performance in waves and associated motion responses, etc. Within this framework, this project has been initiated to further explore the effect of Hull Vane as applied onto large vessels in design and optimisation, resistance reduction, improving the motion response in still water and waves, and eventually exploring full-scale extrapolation methods. In the paper Hull Vane with Rhodes St. Gense 32 foil section is designed and applied on an existing 1:51 DTMB 5415 hull form. The test campaign has been conducted with different attack angles and foil locations under both still water and waves. After the experiments, two different full-scale extrapolation approaches have been discussed and applied to estimate the full-scale performance using Hull Vane.

## **2 Description of Experimental Model Test**

### **2.1 Experimental Setup**

#### **2.1.1 Brief Description of the Towing Tank Facility**

The emphasis of this study is to perform a systematic research of design optimisation and experimental validation of the Hull Vane in order to further explore and determine how Hull Vane effects ship performance in different marine environments. The experiments for this research were performed in the towing tank facility in the Kelvin Hydrodynamics Laboratory (KHL) at the University of Strathclyde.

The principal dimension of the towing tank is 76m x 4.6m x 2.5 m. The facility is equipped with a computer-controlled digital drive carriage with max speed 5m/s, a variable-water-depth computer-controlled four-flap absorbing wavemaker generating regular/irregular waves over 0.5m height, and high quality variable-water-depth sloping beach, with reflection coefficient typically less than 5% over frequency range of interest.

The resistance is measured by a tension-compression load cell. Meanwhile the dynamic trim and sinkage are acquired by two Linear Variable Displacement Transformers (LVDTs) fitted to the bow and stern of the models. All the data is collected by a 16-bit system with the sampling rate, 137 Hz.

#### **2.1.2 Ship Model Selection**

To evaluate the influence of the Hull Vane on the large displacement vessels, a well-known benchmark hull form, the DTMB5415 destroyer model, was selected. DTMB5415 is a 142-meter-long conceptual model, an open-to-public early concept of the DDG-51 known as the Arleigh Burke class destroyer. The hull geometry includes sonar dome and the transom stern. The 3D CAD model has been presented in Fig.5 and a testing model in 1:51 scale was manufactured in fibreglass epoxy by the Kelvin Hydrodynamics Laboratories. Full scale and model scale particulars are given in the Table 2.

### **2.1.3 Design of Hull Vane**

Foil section was selected based on the estimated Reynolds number ( $R_n=0.1e+6$ ) under the operating conditions. With the experiences from previous studies, the utilization of profiles similar to NACA 4412 with curved bottom surface is favourable to achieve a high lift/drag ratio (CL/CD). For the simplicity of manufacturing, Rhodes St. Gense 32 profile with the flat bottom edge (Fig.6) was selected and manufactured in balsa wood along with the wooden streamlined struts (Fig. 7). The lift/drag ratio, CL/CD, of the foil simulated in XFOIL is presented in the Fig. 8 under  $R_n=0.1e+6$ .

According to the previous researches, the chord length and the span of the foil model are set to 0.055m and 0.27m respectively. Then, the foil was fixed onto the vessel with an aluminium bracket with precision-drilled holes for varying the locations marked in the figure as shown in Fig. 9 and the detail is shown in Table 3.

## **2.2 Test Matrix**

During the experiment, model was towed in the range of speeds corresponding to the full-scale speeds from 18 to 30 knots. All of the tests conducted under the still water conditions were repeated under the wave conditions using the regular waves with a constant frequency at 0.75Hz (9.53 sec and 142m length in full scale) and a varying wave heights from 2 to 4cm, reflecting to 1-2m wave height in full scale. The angle of attack (AoA) was also systematically varied during the test with the initial angle of attack of 2 degrees. In total 180 tests have been conducted and has been summarised and shown in Table 4.

## **2.3 Test Procedure**

The test was carried out under the guidance of the standard ITTC guidelines. Model was towed in purely upright conditions, with the Hull Vane being fitted as the appendage. During the test, the model was free to heave, pitch and roll, with the towing post exerting horizontal force only. Measuring equipment was calibrated to the standards of Kelvin Hydrodynamics Laboratory using set weights for the load cell and calibrated step plate for both LVDTs. The readings of resistance, trim and sinkage were recorded by highest quality equipment and data acquisition software.

Investigation of uncertainty was carried out in respect of resistance and trim measurements, according to ITTC-Recommended Procedures and Guidelines, Uncertainty Analysis Instrument Calibration, 7.5-01-03-01. The measured standard error of estimate is 0.056N for the load cell that has been used for the test, which presents a high accuracy of measurement(ITTC, 2008).

## 3 Experimental Results and Discussions

### 3.1 Test in Calm Sea

#### 3.1.1 Resistance Performance in Still Water

Fig. 10 shows the total resistance coefficient ( $C_T$ ) of bare hull and hull fitted with the Hull Vane at various locations and AoAs in still water.

The total resistance coefficient is obtained from the following Equation 1.

$$C_T = \frac{R}{0.5\rho V_c^2 A} \quad \text{Equation 1}$$

where  $R$  is the measured total resistance, N;  $\rho$  is water density, kg/m<sup>3</sup>;  $V_c$  is the carriage velocity, m/s; and  $A$  is the wet surface of the model under still condition, m<sup>2</sup>. Wetted surface area under still condition will be increased due to the Hull Vane.

Initially, slight increase in  $C_T$  at lower  $Fn$  can be observed in all the situations when the Hull Vane is installed.  $C_T$  of hull with Hull Vane starts to decrease and become lower than that of bare hull after the Froude number exceeds 0.33, except when the vane is fitted with  $-17^\circ$  and  $30^\circ$  AoAs. For the extreme AoAs,  $-17$  and  $30$  degrees, drastic increase of  $C_T$  is observed throughout the full range of speeds.

Fig. 11 shows the comparison of  $C_T$  between Hull Vane and the bare hull under the calm sea condition. Maximum 6.4% reduction in  $C_T$  can be observed when the foil is fitted to Location 1 with  $2^\circ$  AOA at  $Fn=0.397$ . Fig. 11 also indicates that the change of  $C_T$  is highly dependent on the locations and AoAs. Location 1 provides overall the best and consistent performance.

Due to the increase of wetted surface area,  $C_T$  comparison might not reflective to the total resistance; therefore, further comparison has been conducted to compare the resistance itself. Fig. 12 shows percentage changes in the resistance with the varying Froude number. It can be observed that for  $Fn>0.339$ , Hull Vane at the location 1 provides constant reduction in resistance with maximum 3.8% reduction at  $Fn=0.397$ .

### 3.1.2 Motion Response in Still Water

Together with the resistance performance, the motions of the vessels are also recorded to analyse what is the effect on the motion and the reason of resistance reduction. Fig.13 shows trim response of the model at all test setups, the trim response is expressed in degrees and the negative degree represents downward movement of the bow.

Except when the hull vane was installed at  $-30^\circ$  AoA, deployment of the Hull Vane will induce bow down motion, which varies depending on the locations and the angles of attack of the foil. The largest trim can reach  $-0.547^\circ$ . It has to be mentioned that the difference in the trim between three locations is marginal, thus it can be assumed that the effect on trim is not strictly dependant on the longitudinal or vertical location of the foil. However, it is clearly visible that the variation of the AoA can significantly impact on the trim angle of the vessel. Negative AoA will reduce the trim of the vessel. And extreme AoA, either negative or positive, can cause very high trim throughout all the speeds. On the other hand, as seen in the resistance performance, extreme trim can lead to high resistance throughout the whole speed region.

Meanwhile, Fig.14 represents the sinkage generated by bare model hull and models with Hull Vane. It can be observed that with the increase of the speed, the vessel in all of the configurations is gradually experiencing a sinkage. Sinkage will cause increase of draft and hull wetted surface, which contributes to the increase of the total resistance. And Hull Vane can help to reduce the sinkage. But the difference between the measured sinkage caused by hull vane in different locations is also marginal, suggesting that effect of the Hull Vane locations on the sinkage is not significant. However, the result shows altering the AoA has a more significant influence on the sinkage of the DTMB5415 model. 5% reduction in sinkage can be observed at the  $Fn=0.42$  for vane at  $-6$  degrees angle. When the angle of attack is set to  $17$  degrees, the vessel sinkage reduced by 15%. However, as seen from previous test, it introduces significant resistance.

Apart from the measured data of the resistance and motion response of the vessel, the influence of deployment of the Hull Vane can be visually observed. In Fig.15, it shows the wave pattern behind the hull observed from the top view. The change of the

wake wave pattern is clearly visible when the Hull Vane is fitted. Very turbulent wave can be observed after the bare hull while the wave is much smoother when fitted with the Hull Vane, indicating the wave making resistance can be reduced by the Hull Vane.

## 3.2 Test in Waves

### 3.2.1 Resistance Performance in Waves

Number of tests were performed in the regular wave head seas. The time average resistance were analysed. Fig.16 shows the values of total resistance coefficients of bare hull and hull with Hull Vanes under 0.02m and 0.03m high regular waves with 0.75Hz against two different Froude numbers.

At the lower speed ( $Fn=0.248$ ), change of  $C_T$  caused by Hull Vane is very limited. Fig.17 shows that  $C_T$  can increase by up to 2% when the vane is at the location 3 in 0.02m high wave. Minor  $C_T$  reduction is noticed when the vane is in location 2 and the reduction varies are 0.2% and 1% in 0.02 and 0.03m wave respectively. At the higher speed region, the  $C_T$  reduction is obvious and the effect become more obvious with the increasing wave height. When the wave is 0.03m high, Hull Vane at location 2 can reduce  $C_T$  by up to 8.1%.

However, it is worth noting that due to change in the wetted surface area, the  $C_T$  doesn't fully characterise the variation in the resistance. Therefore, likewise in calm sea, Fig.18 separately presents the percentage change in the total resistance in model scale experiment for 0.02 and 0.03m waves. Similar trend can be observed but in a lower magnitude with maximum 5.5% resistance reduction achieved in location 2.

Fig.19 shows the  $C_T$  of the bare hull and the model fitted with the Hull Vane at various locations as well as various AoAs in location 1 under 0.04m high wave (Representing 2m wave in full scale, about Sea State 4). Firstly, it can be noticed that two vanes with extreme AoAs introduced significant increase of  $C_T$  which is up to 25%. But in majority of the conditions, the Hull Vane resulted in the reduction of  $C_T$  at all of the locations when the AOA is moderate, the highest  $C_T$  reduction in waves can reach 9.8%.

### 3.2.2 Motion Response in Waves

The motion response analysis in waves are focusing on the dynamic trim analysis since it is of highly concern of vessels comfort and operability.

- **Time Averaged Response in Dynamic Trim**

In order to explore what is the reason of resistance reduction in wave, firstly the time averaged motion responses have been analysed. Fig.20 represents the measured mean trim in degrees at various wave heights when the Froude number is 0.248 and 0.413 respectively. The significant effect of the Hull Vane can be observed when the foil is fitted. The trim of hull with foil fixed at location 2 and location 3 can be reduced by about 20% in different waves and different speed. Fig. 21 represents the effect of location and AoAs of vane on the mean trim angle under the highest 0.04m wave, which shows deployment of the Hull Vane at any tested location can reduce mean trim in waves, but the change of AoAs only can cause the marginal change except the extremes.

- **Dynamic Trim Response in Frequency Domain**

From Fig. 22 to Fig. 27, frequency domain analysis has been performed to analyse the response of dynamic trim using FFT analysis. It can be observed that the application of the Hull Vane at any locations and any AoAs can effectively damp the trimming response of the vessel, reduce the amplitude of trim and spread in response away from the encounter frequency to a wider range of frequencies. In general, 20-30% reduction of motion response can be achieved. It can be concluded that the Hull Vane effect on the motion response depends on the speed of vessel, the wave height and the location of the vane, and the vane can reduce the trim response significantly and improve the operability of vessel.

For example, Fig.26 and Fig.27 represent the trim response in the frequency domain in 0.04m waves when the Froude number is 0.248 and 0.413 respectively. In comparison to the bare hull, Hull Vane fixed at the location 2 can reduce the response by up to 25% when the at the  $F_n=0.248$ . At the same speed, the results of Hull Vane fixed at location 1 show that the alternation of the AoA can further reduce the trim response of hull. During the experiment at the  $F_n=0.413$ , trim response can be

reduced by up to 26% when the foil is at location 3 when the encounter frequency is 1.52Hz.

## **4 Full-scale Resistance Extrapolation**

Currently the prediction of full-scale performance for Energy Saving Devices is still under development. There is no official guidelines in the resistance extrapolation methods, nor in the propulsion. The difficulty lies on the complicity of flow developed around the ESDs and its interactions on the hull flow. In this paper, exploration has been conducted using two different extrapolation methods to predict the possible full-scale performance.

### **4.1 Method I: Impact on Form Factor**

Method I considers the Hull Vane to have direct impact on the flow around the vessel. So the discussion is around the change of form factor by Hull Vane by taking Hull Vane as a part of the hull. The reason for using this method is because, as it can be observed during the test, the wave pattern in the stern area has been significantly changed by this ESD. So the change in the form factor,  $k$ , is expected. However during the test, the priority was focused on the performance in model scale. Therefore  $(1+k)$  was not measured during to the test.

To tackle this issue, CFD method based on Reynolds Averaged Navier Stokes (RANS) was then used to estimate the  $1+k$  values in both bare hull model and with Hull Vane at location 1 (most efficient).

The RANS computations are performed to estimate the form factor values with the most common two-equation turbulence model, The Shear stress transport  $k-\omega$  (SST). SST  $k-\omega$  turbulence model(Menter, 1994) is an improved version of the standard  $k-\omega$  model(Wilcox, 1988). The model includes a cross-diffusion term in the  $\omega$  equation along with a blending function which avoid sensitivity of the standard  $k-\omega$  model to free stream boundary conditions. The modification caused the new model to behave identical to the standard  $k-\epsilon$  for free shear flows. The SST model also includes a new definition of the turbulent viscosity improving its prediction capability for boundary layer flows with adverse pressure gradients.

The computational mesh was generated with a well-known cut-cell technique with in total 0.5 million cells which is a type of non-matching block-unstructured volume

mesh generation method. The trimmed cell mesher provides a robust and efficient method of producing a high-quality grid. By using the advantage of the working at slow speeds, the  $y^+$  value of the first cell adjacent to the outer surface of the hull and the appendages was kept under 5. Six layers of grid inflation was used in the boundary layer to model near wall region. In order to check grid dependency of the computational results, additional computations were carried out with different mesh densities at 0.5 m/s. The  $y^+$  value of the first cell was kept constant and grid size systematically changed at each direction around the hull and the Hull Vane, independently. The negligible difference (less than 1% for the acting forces on the Hull Vane and total drag force) between the results of different mesh structures.

In the simulations, steady, incompressible RANS equations were solved. Star CCM+ 13.04 software package was used for the mesh generation and the computations. The inlet boundary condition is  $1.5L_{pp}$  upwards from the ship and the outlet is  $2L_{pp}$  downwards from the ship. Considering the symmetry of the hull geometry, simulations were performed by using half ship in model scale without the free surface. A view of the generated mesh is shown in Fig. 28. The ambient turbulence conditions in the domain were introduced with intensity of 0.01 to replicate the turbulence simulators at the bow of the model.

The RANS and related transport equations were solved by finite volume technique with a segregated algorithm (Blazek, 2015). For the pressure-velocity coupling, standard pressure correction procedure, SIMPLE, was used (Patankar and Spalding, 1983). The iterations were run until the residuals dropped to a level of  $10^{-6}$  while total drag and the forces on the Hull Vane checked in order to decide whether the convergence was achieved.

$(1+k)$  was found to be 1.126 for the bare hull and coincide with the value 1.104 obtained from the previous tests in KHL. CFD analysis for the model equipped with the Hull Vane at the Location 1 was performed under the same simulation conditions and then  $(1+k)$  was obtained to be 1.193 for this configuration.

Then extrapolations for both bare hull and hull with vane were carried out by using the standard ITTC procedure for resistance estimation, as shown in Equation 2.

$$C_T = (1 + k)C_F + C_W + C_A + \Delta C_F$$

**Equation 2**

where  $C_F$  is the frictional resistance coefficient which is based on ITTC-1957 correlation line,  $C_W$  is the wave making resistance coefficient calculated from the model scale,  $C_A$  is a correlation allowance for different facilities recommended by 19th ITTC and  $\Delta C_F$  is a roughness allowance proposed by 19th ITTC.

Total resistance was then calculated with the following Equation 3.

$$R_T = \frac{1}{2}\rho V^2 S_W C_T$$

**Equation 3**

where  $\rho$  is a water density,  $V$  is a speed of a full-scale ship in m/s,  $S_W$  is a wet surface and  $C_T$  is the total resistance coefficient.

## 4.2 Method II: Hull Vane as Appendages

Besides Method I, discussion is happening around whether Hull Vane shall be taken just as an appendage, like a rudder, as it is very close to the rudder position and stays behind and away from the hull. Therefore Method II is proposed to assume that the Hull Vane is far enough from the vessel and has no effect on the flow around the stern. Thus, the form factor won't be changed, and Hull Vane is treated as an appendage. The decomposition of the resistance coefficients can be written as Equation 4.

$$C_T = (1 + k)C_F + C_W + C_A + \Delta C_F + C_{APP}$$

**Equation 4**

where  $C_{APP}$  is the appendage resistance coefficient.

To investigate the appendage resistance coefficient in different Reynolds Numbers, XFOIL software package was utilized to analyse the drag coefficient  $C_d$  of the foil section. The  $C_d$  of foil section in model scale has been calculated to be 0.0178 with  $Re=0.1 \times 10^6$ , while the  $C_d$  in full scale being 0.0064 with  $Re=36 \times 10^6$ .

The appendage coefficients for model scale and full scale was obtained using the Equation 5.

$$C_{A_{pp}} = \frac{C_d \bar{c} B}{S_w}$$

**Equation 5**

where  $C_d$  is the foil section drag coefficient at different Reynolds numbers,  $\bar{c}$  is the mean chord length, B is a foil span and  $S_w$  is the wetted surface area of hull with the Hull Vane.

### **4.3 Full-scale Resistance Extrapolation Results and Discussions**

Location 1 was selected for the full-scale analysis, due to its most significant effect on the resistance reduction at the higher speed range. Fig. 29 represents full-scale total resistance coefficient ( $C_T$ ) against the Froude number for bare hull and with Hull Vane using two extrapolation methods.

The  $C_T$  of the bare hull and the two  $C_T$  predicted based on the above extrapolation methods for the one with Hull Vanes can be compared in Fig. 29 and the comparison in percentage is shown in Fig. 30. It can be seen that both methods predict similar results for full-scale resistance performance. The maximum difference between two methods is within the region of 1%. At the lower speed range ( $0.248 < Fn < 0.281$ ), Method II estimates higher reduction in the  $C_T$ . When the Froude number is over 0.298, Method I evaluates more significant reduction in  $C_T$  comparing to the Method II.

The change in the full-scale resistance predicted by using these two extrapolation approaches is presented in the Fig. 31. Both methods predict maximum around 10% resistance reduction in full-scale application.

## 5 Conclusions

This paper investigates the effect of underwater stern foil, Hull Vane, with the application in different locations and angles of attack on the resistance performance and motion response for large displacement ships. The following conclusions can be made:

1. The calm water resistance test results confirm that the Hull Vane is an effective Energy Saving Device for large displacement vessels particularly in high speeds with maximum 6.4% reduction in  $C_T$  and 3.7% reduction in total resistance observed in model-scale tests. The reduction is accredited to the reduced sinkage and suppression of stern wave, as observed during the tests.
2. Reduced wave added resistance and motion response can be observed in the wave tests for the model with Hull Vane in both time-averaged results and oscillation amplitudes. Up to 26% oscillating trim amplitude can be reduced as observed in the tests due to the damping effect created by the Hull Vane. And the biggest influence is achieved by alternation in the longitudinal positions.
3. Two full-scale extrapolation methods for Hull Vane are proposed explored based on different assumptions. One is assuming that Hull Vane is impacting on the form factor while the other takes Hull Vane as an appendage. However both methods predict close results in full-scale resistance and about 10% resistance reduction can be expected in full-scale application.

## Acknowledgment

The authors would like to express sincere gratitude to the support received from the staff in Kelvin Hydrodynamic Lab. Without whom, the study cannot be completed. Thanks to their generous support for student projects.

## References

- Allema, J., 2005. Intercepting the Interceptor. Marin Report No 86 September 2005 6-7.
- Andrew, A., Prasanta K Sahoo; Sudarshanaram Ramakrishnan, 2015. Resistance Characteristics For High-Speed Hull Forms with Vanes.
- Avci, A.G., Barlas, B., Ölçer, A.I., 2018. An Investigation of Fuel Efficiency in High Speed Vessels by Using Interceptors, Trends and Challenges in Maritime Energy Management. Springer, pp. 127-141.
- Blazek, J., 2015. Computational fluid dynamics: principles and applications. Butterworth-Heinemann.
- Bøckmann, E., 2015. Wave propulsion of ships.
- Bøckmann, E., Steen, S., 2013. The effect of a fixed foil on ship propulsion and motions, Proceedings of the Third International Symposium on Marine Propulsors (SMP2013), pp. 553-561.
- Bouckaert, B., 2018. An underwater spoiler on a warship: why, when and how? Zeszyty Naukowe Akademii Marynarki Wojennej 59.
- Bouckaert, B., Uithof, K., Moerke, N., van Oossanen, P., 2016. Hull Vane® on 108m Holland-Class OPVs: Effects on Fuel Consumption and Seakeeping, Proceeding of MAST Conference.
- Bowker, J., Townsend, N., Tan, M., Sheno, R., 2015. Experimental study of a wave energy scavenging system onboard autonomous surface vessels (ASVs), OCEANS 2015-Genova. IEEE, pp. 1-9.
- Day, A.H., Cooper, C., 2011. An experimental study of interceptors for drag reduction on high-performance sailing yachts. Ocean Engineering 38 (8-9), 983-994.
- ITTC, 2008. Uncertainty analysis instrument calibration (7.5-01-03-01). ITTC–Recommended Procedures and Guidelines.
- Karafiath, G., 2012. Stern End Bulb for Energy Enhancement and Speed Improvement. Journal of Ship Production and Design 28 (4), 172-181.
- Menter, F.R., 1994. Two-equation eddy-viscosity turbulence models for engineering applications. AIAA journal 32 (8), 1598-1605.
- Patankar, S.V., Spalding, D.B., 1983. A calculation procedure for heat, mass and momentum transfer in three-dimensional parabolic flows, Numerical prediction of flow, heat transfer, turbulence and combustion. Elsevier, pp. 54-73.
- PENSA, C., DE LUCA, E.F., 2011. Experimental Study on Interceptor's Effectiveness.
- Suastika, K., Hidayat, A., Riyadi, S., 2017. Effects of the application of a stern foil on ship resistance: A case study of an Orela crew boat. Int. J. Tech 8 (7), 1266-1275.

UITHOF K, B.B., van OOSSANEN P.G, MOERKE N, 2016. Hull Vane ESD on DTMB5415 Destroyer – A CDF Analysis of the Effect on Resistance. MAST Conference 2016, Amsterdam, Netherlands, 2016. 21-23.

Uithof, K., Hagemester, N., Bouckaert, B., van Oossanen, P., Moerke, N., 2016. A systematic comparison of the influence of the Hull Vane®, interceptors, trim wedges, and ballasting on the performance of the 50m AMECRC series# 13 patrol vessel. Proc. Warship.

Wilcox, D.C., 1988. Reassessment of the scale-determining equation for advanced turbulence models. AIAA journal 26 (11), 1299-1310.

## Figures



**Fig. 1 HullVane installed on Themis vessel**



**Fig.2 Interceptors Fitted to High Speed Vessel**



**Fig.3 Stern End Bulb on the Model Scale**



**Fig.4 Bow foil on a model ship**

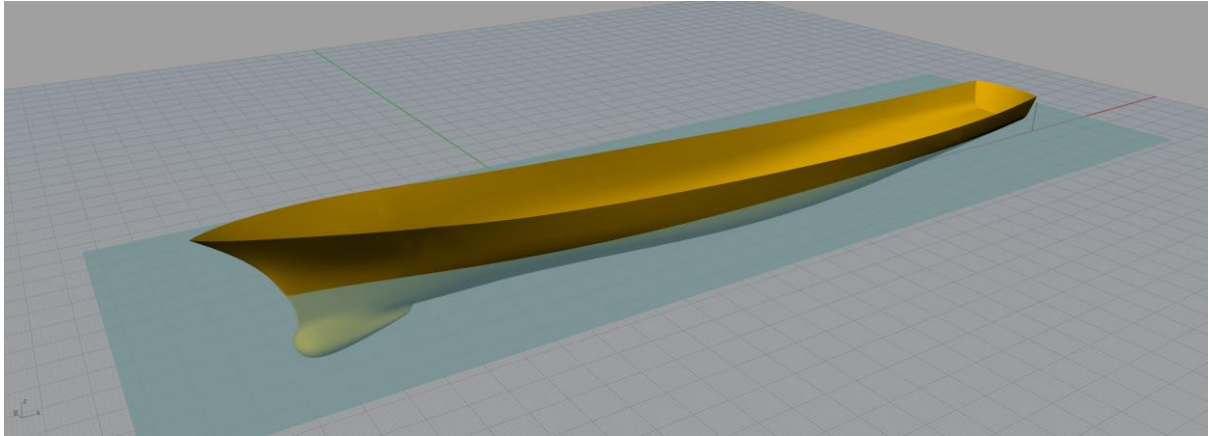


**Fig.5 DTMB5415 CAD model**

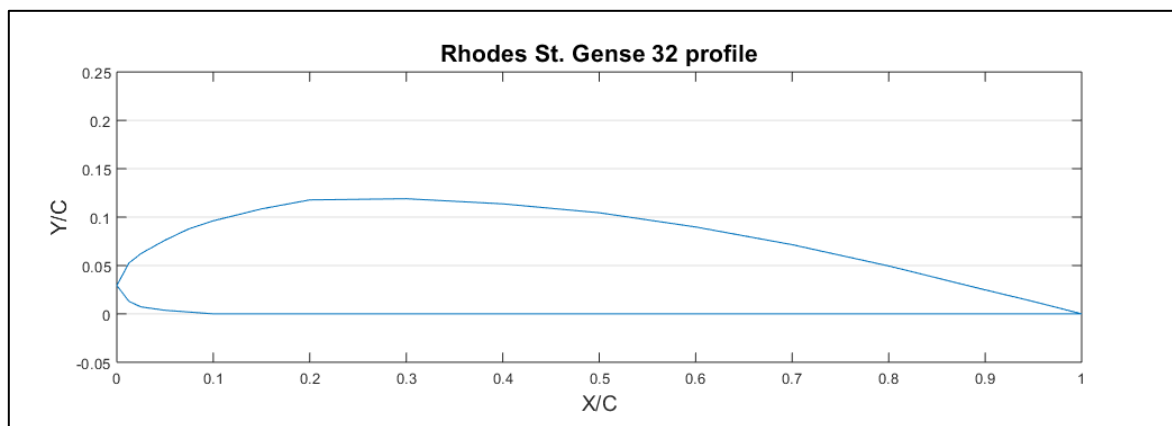


**Fig.6 Rhodes St. Gense 32 profile**



**Fig.7 Manufactured Hull Vane in model scale**

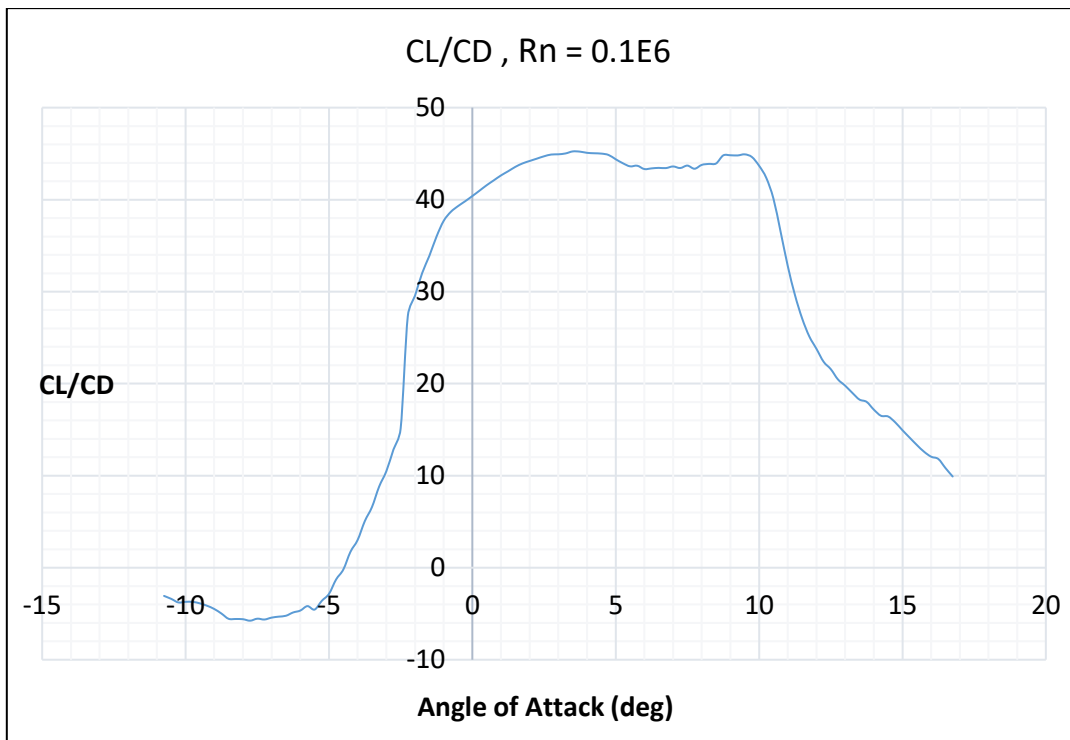


**Fig.8  $C_L/C_D$  against the angle of attack at  $R_n=0.1E6$**

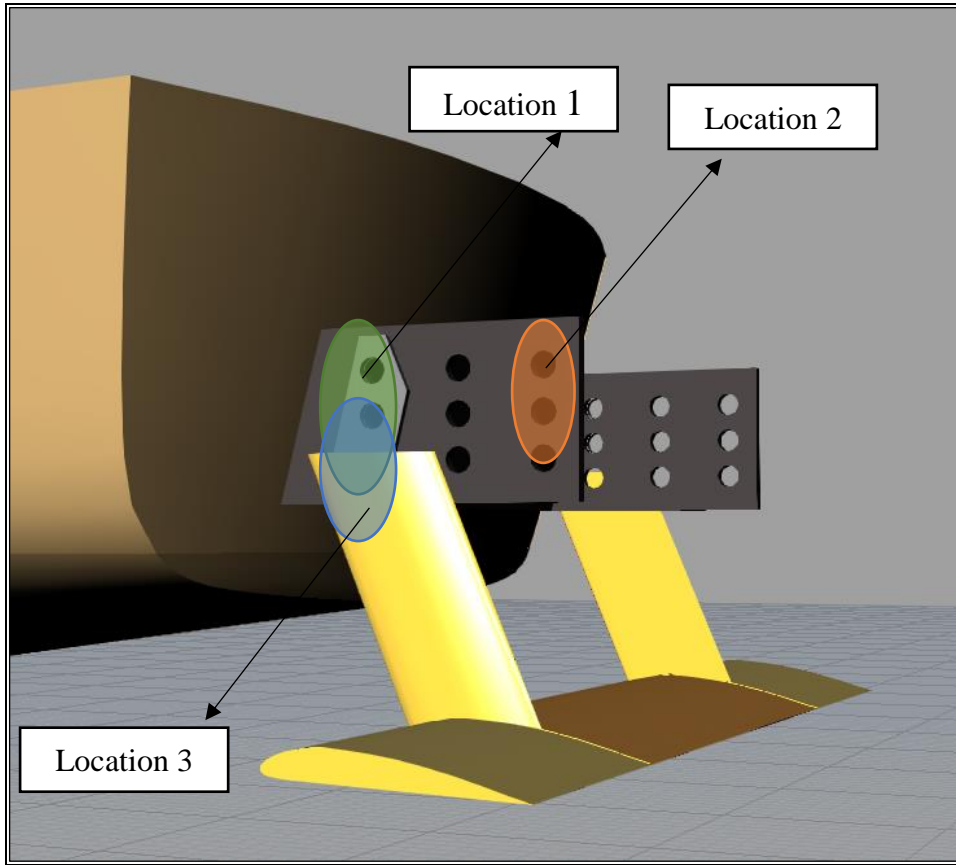


**Fig.9 Hull Vane installation setup**

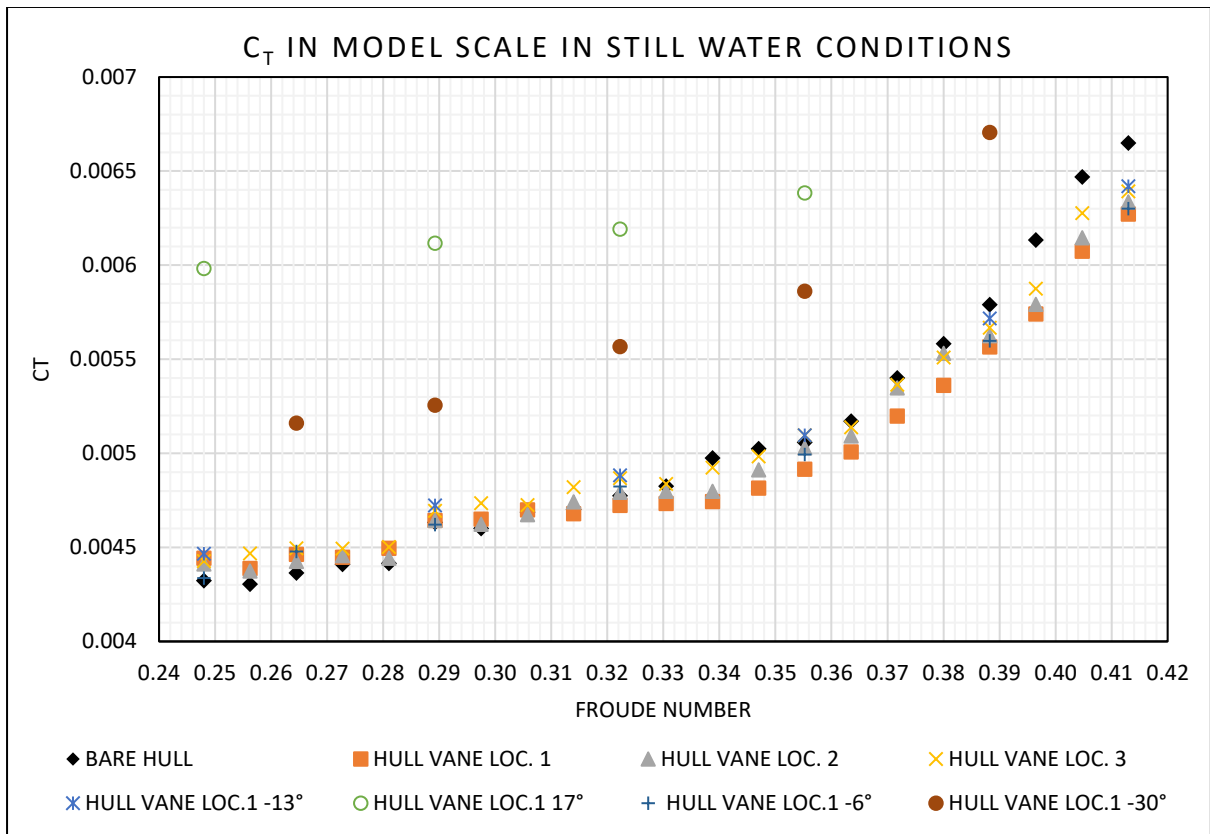


**Fig. 10 Resistance performance in model scale under the still water condition**

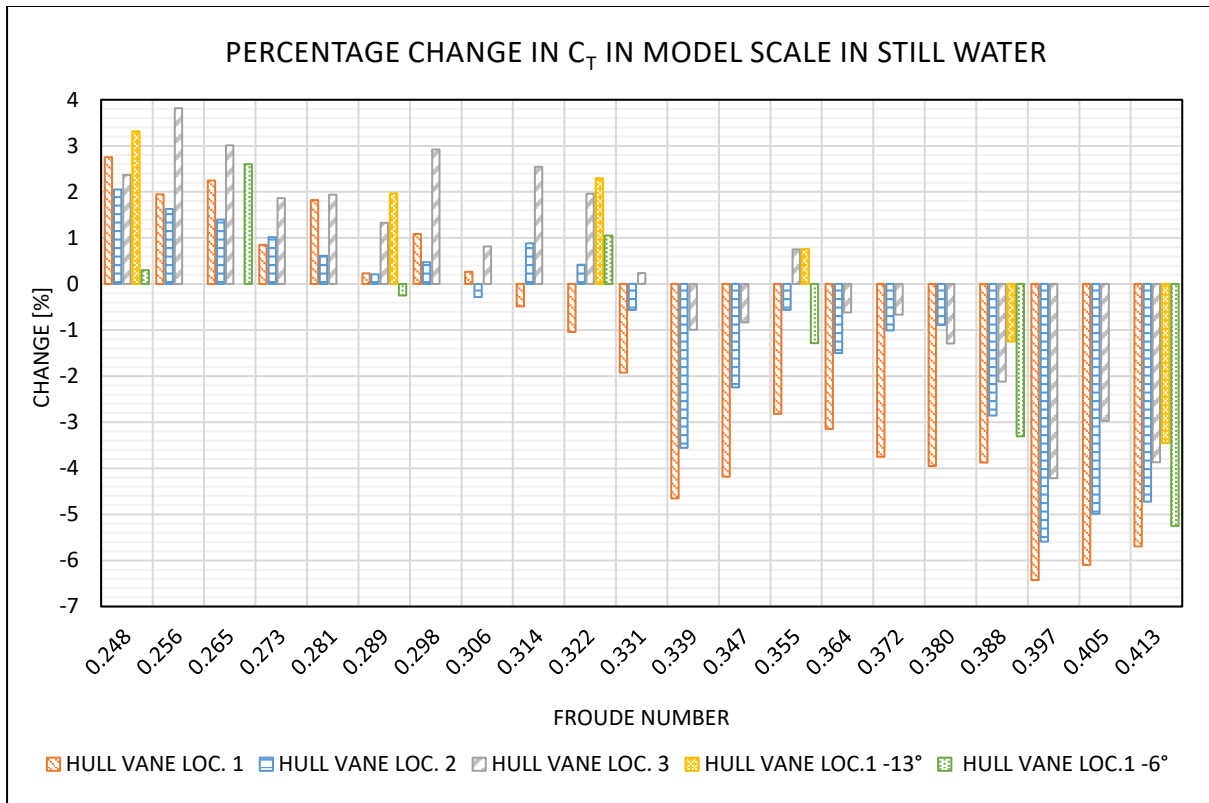


**Fig. 11 Percentage changes in resistance coefficient at model-scale testing**

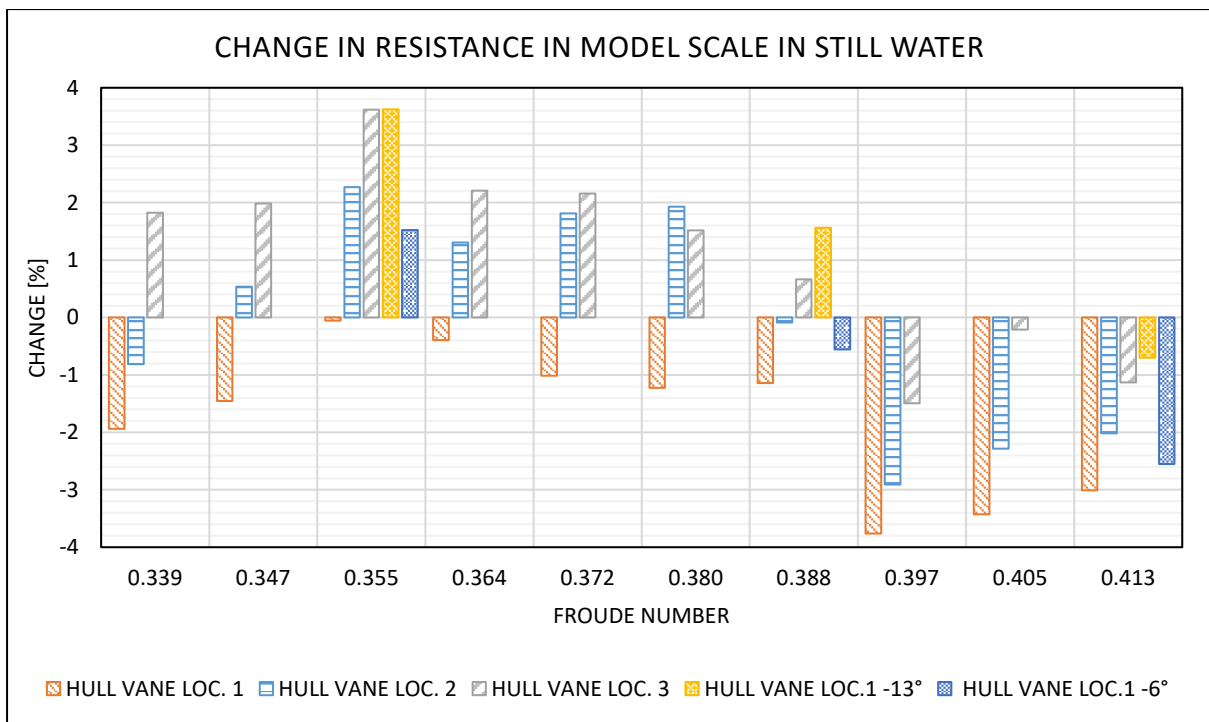


**Fig. 12 Percentage change in the resistance in model-scale**

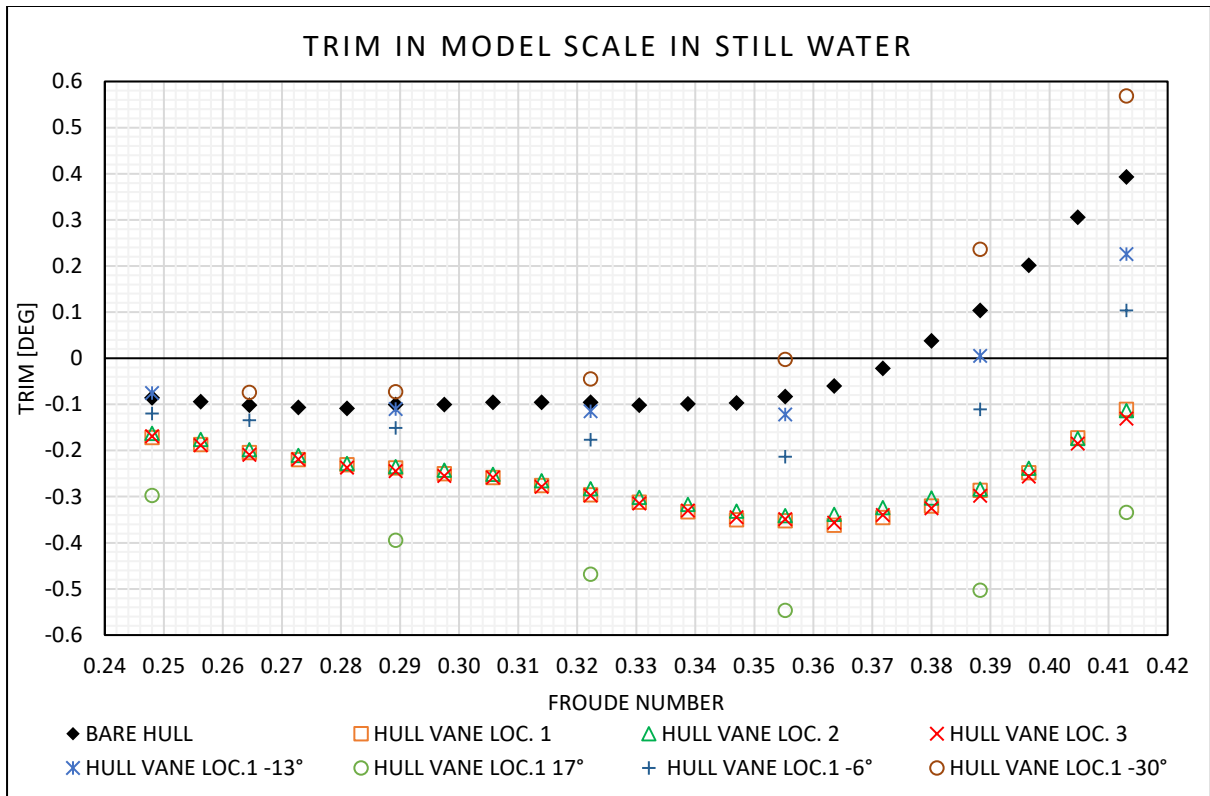


**Fig. 13 Trim response in still water**

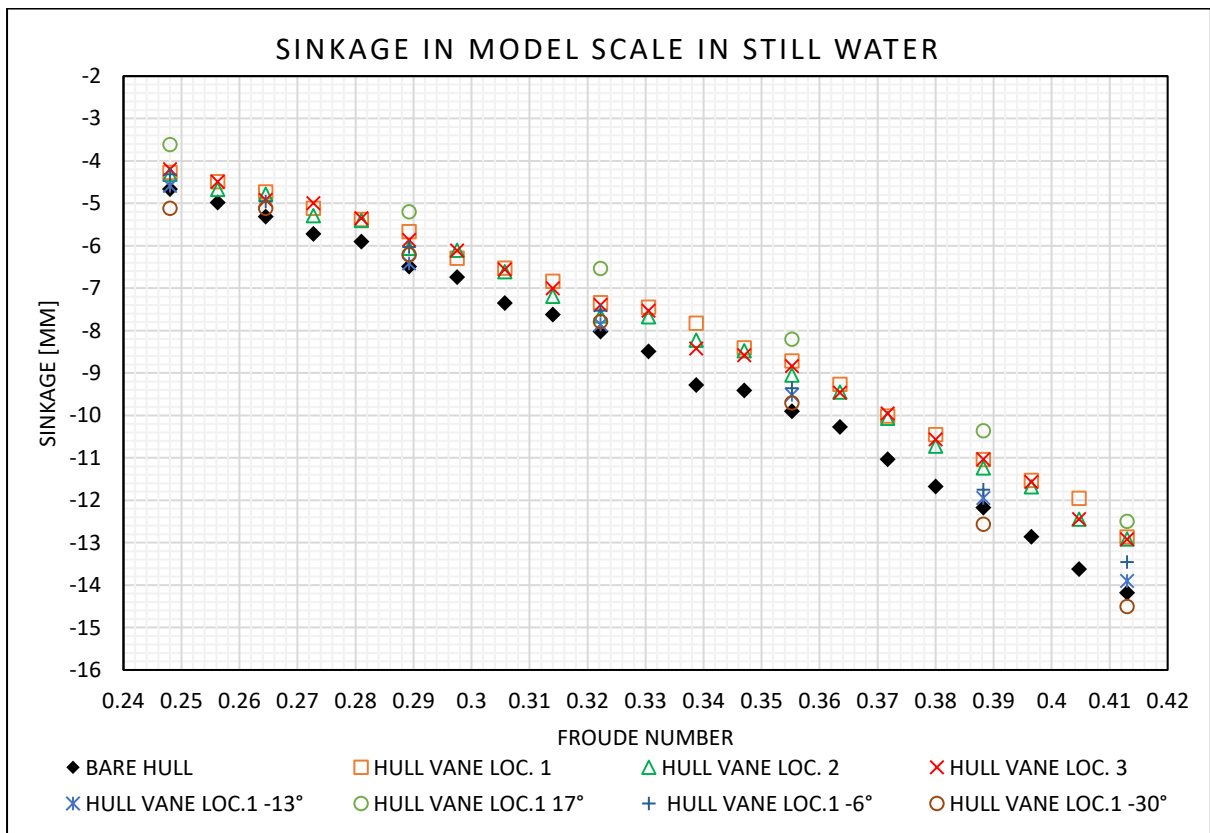


**Fig. 14 Sinkage recorded in experiment for still water condition**

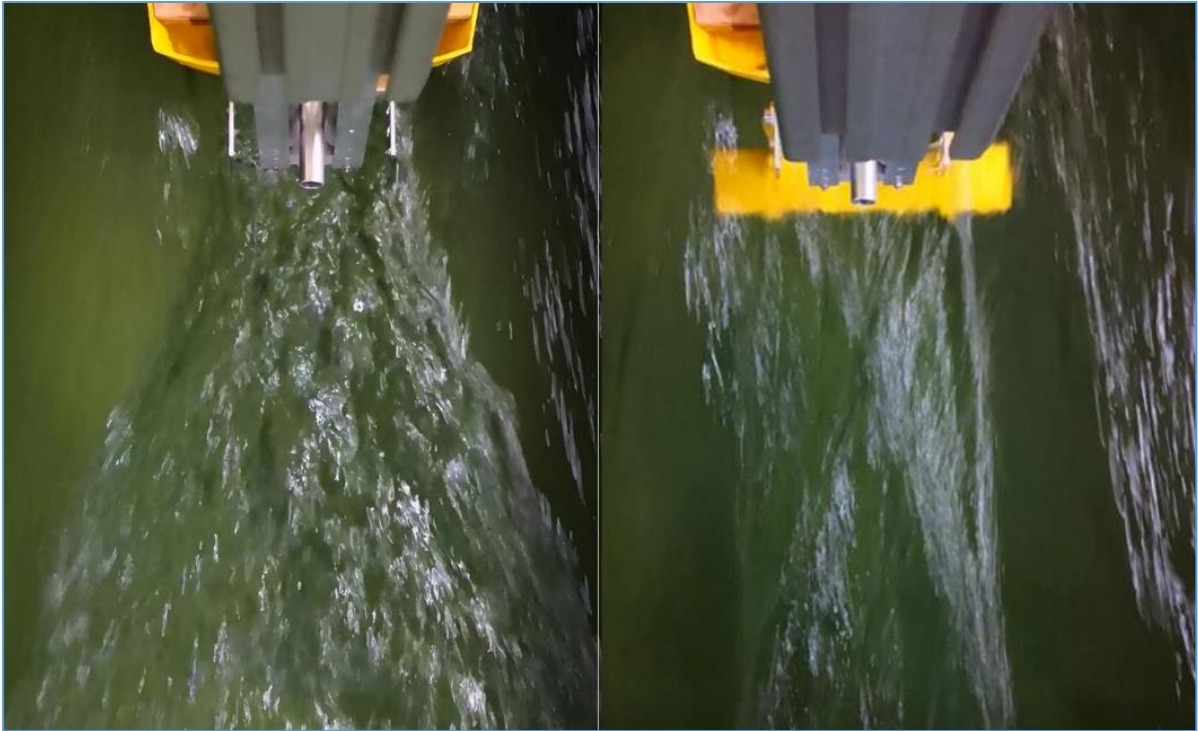


**Fig. 15** Wave pattern behind hull without (left) and with the Hull Vane (right)

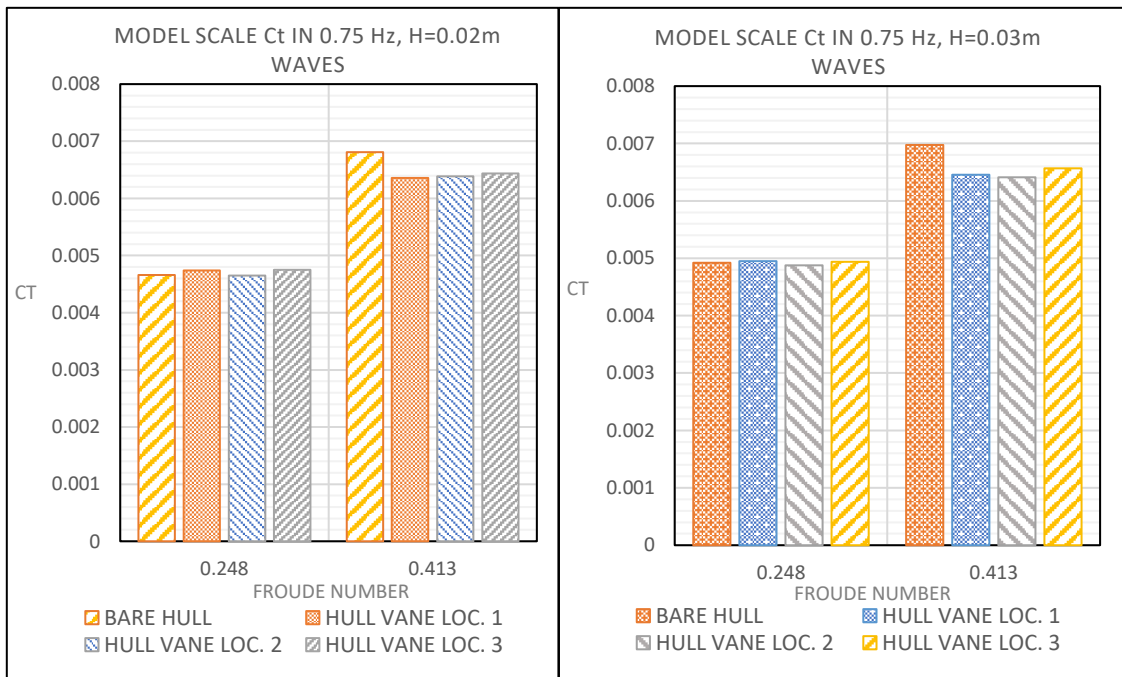


**Fig. 16** Resistance coefficient for model scale in 0.02 and 0.03m waves

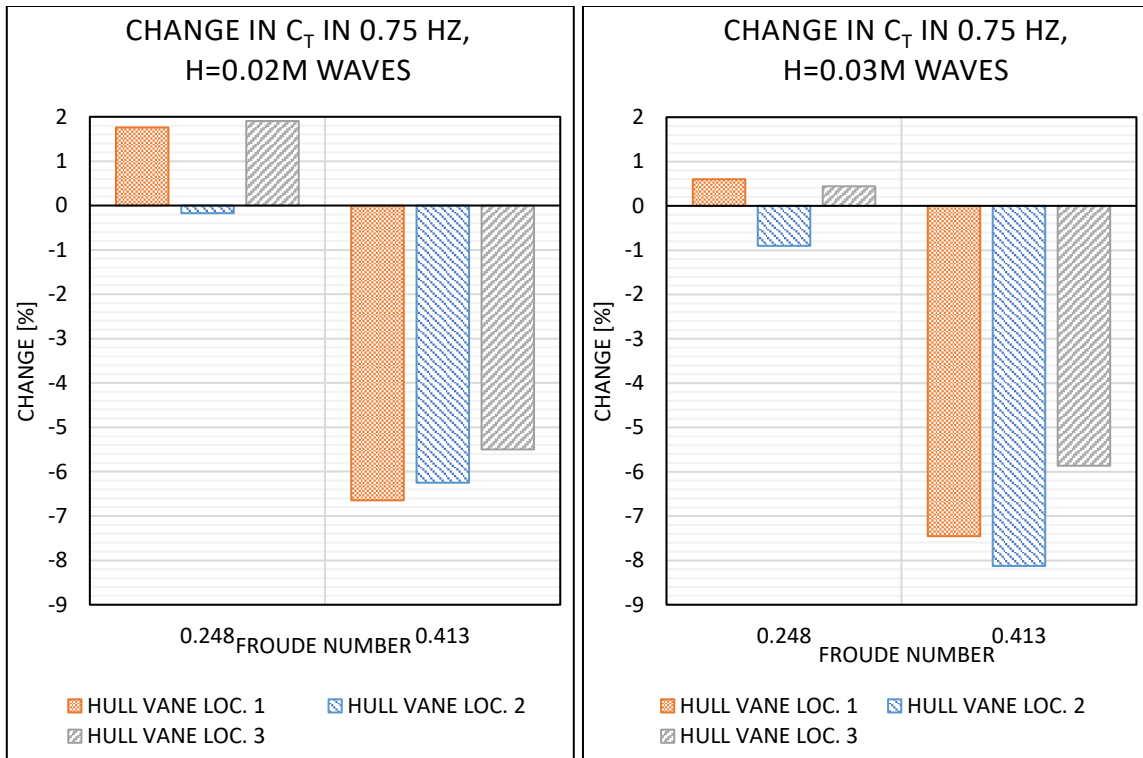


**Fig. 17 Percentage change in  $C_T$  in model scale under waves**

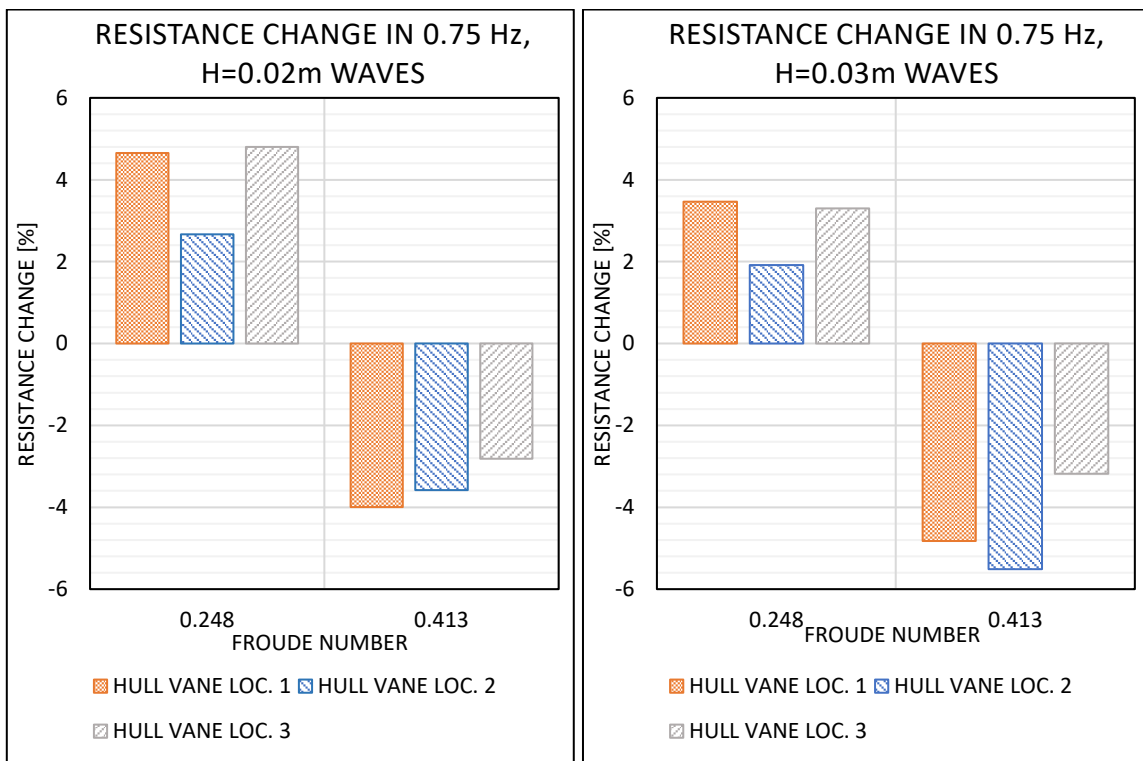


**Fig. 18 Percentage change in resistance due to the waves**

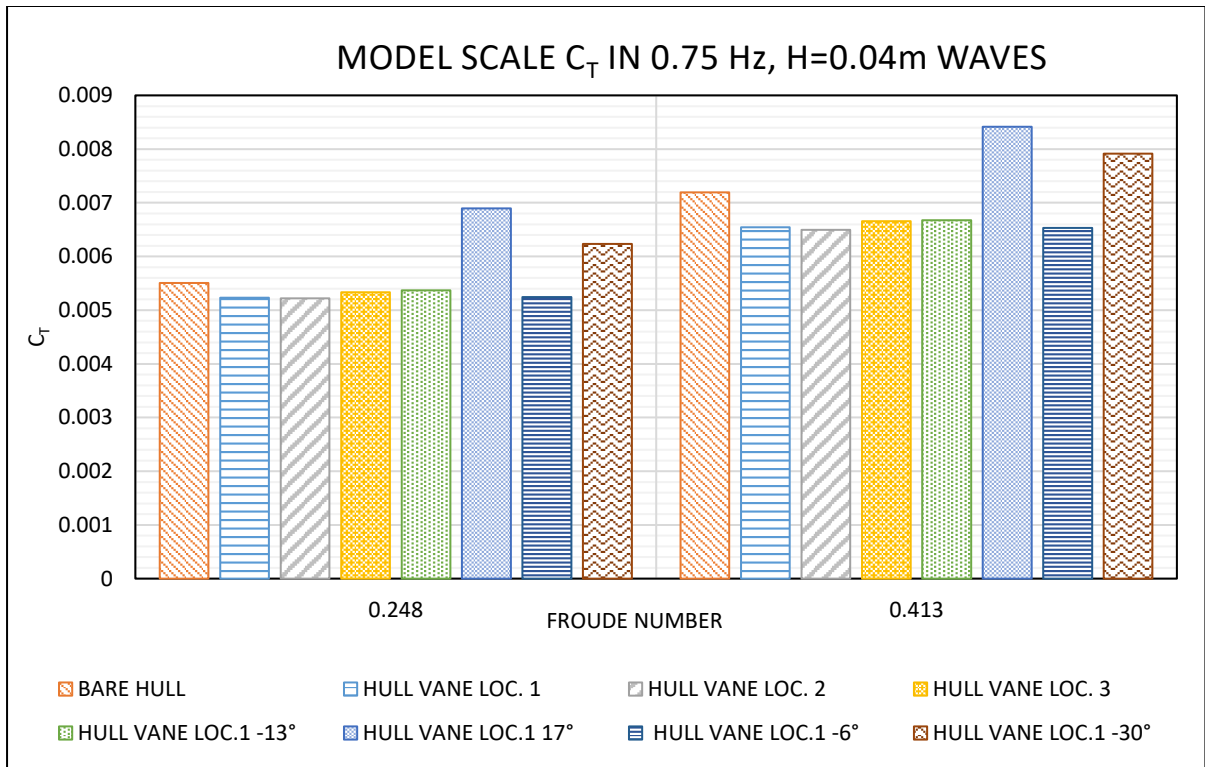


**Fig. 19  $C_T$  variation in model scale in 0.04m wave**

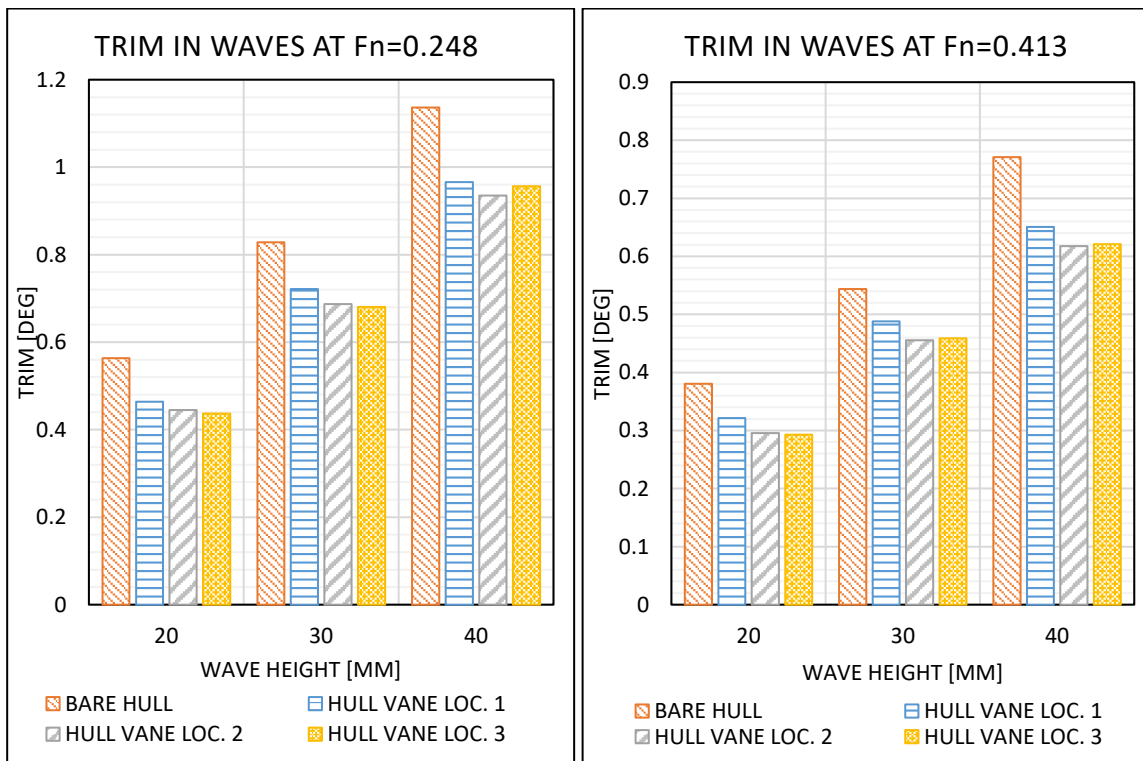


**Fig. 20 Trim in waves at Fn=0.248 (Left) and Fn=0.413 (Right)**

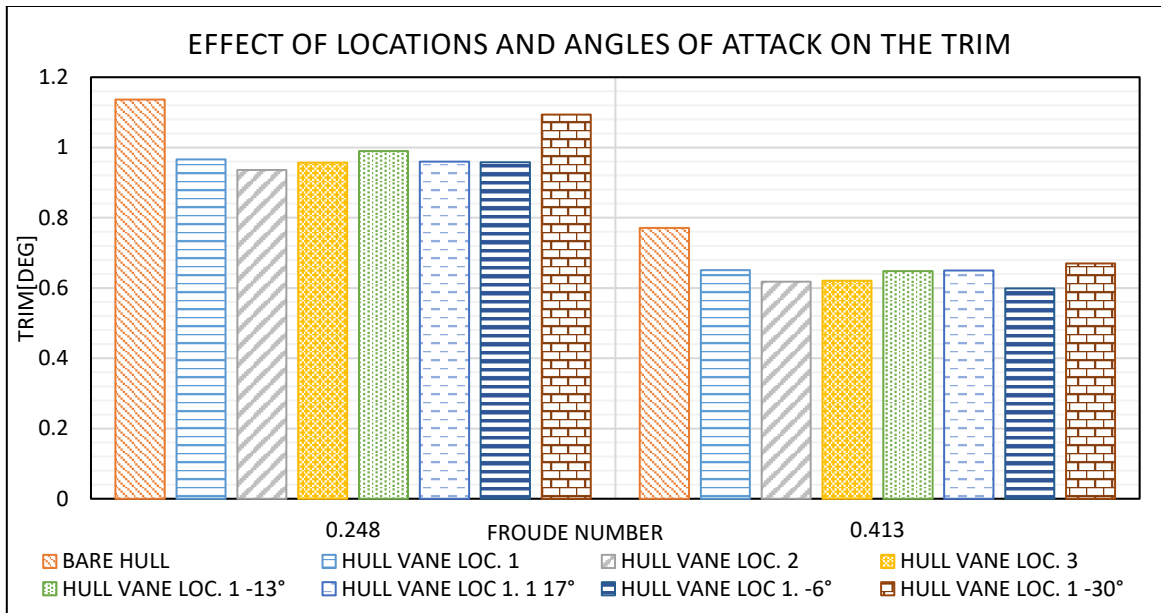


**Fig. 21 Effect of the location and AoA on the trim**

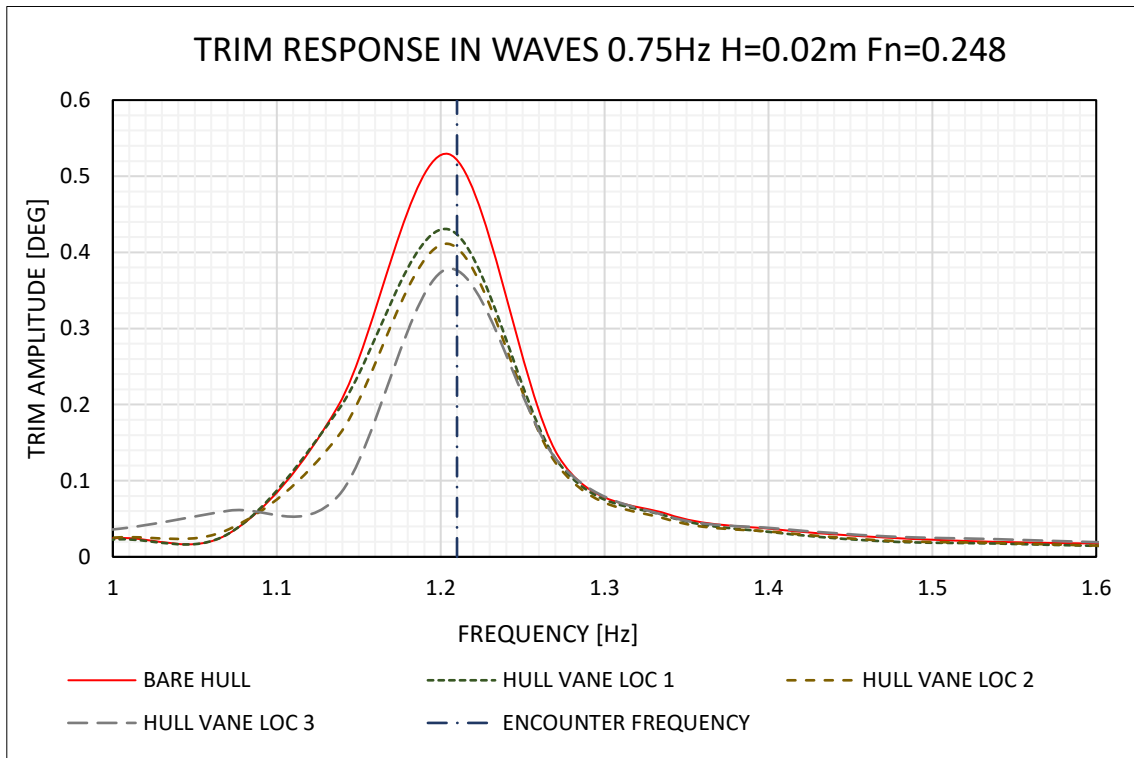


**Fig. 22 Frequency domain trim response in 0.02m wave at Fn=0.248**

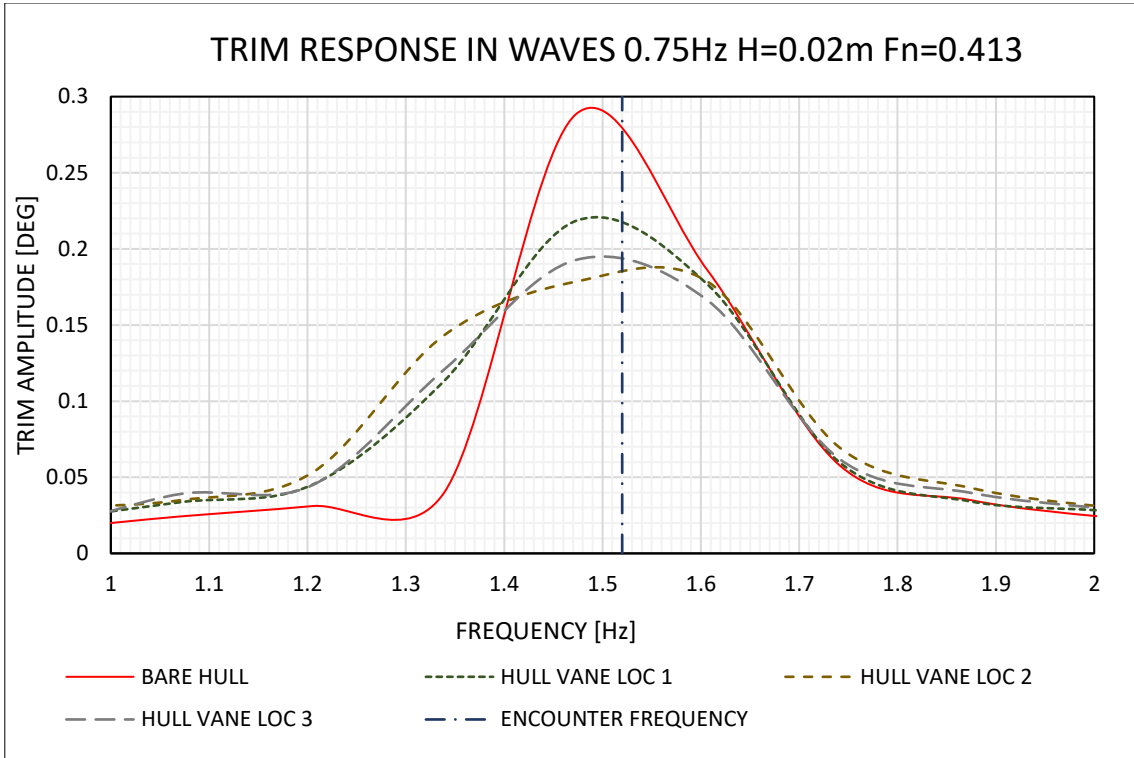


**Fig. 23 Frequency domain trim response in 0.02m wave at Fn=0.413**

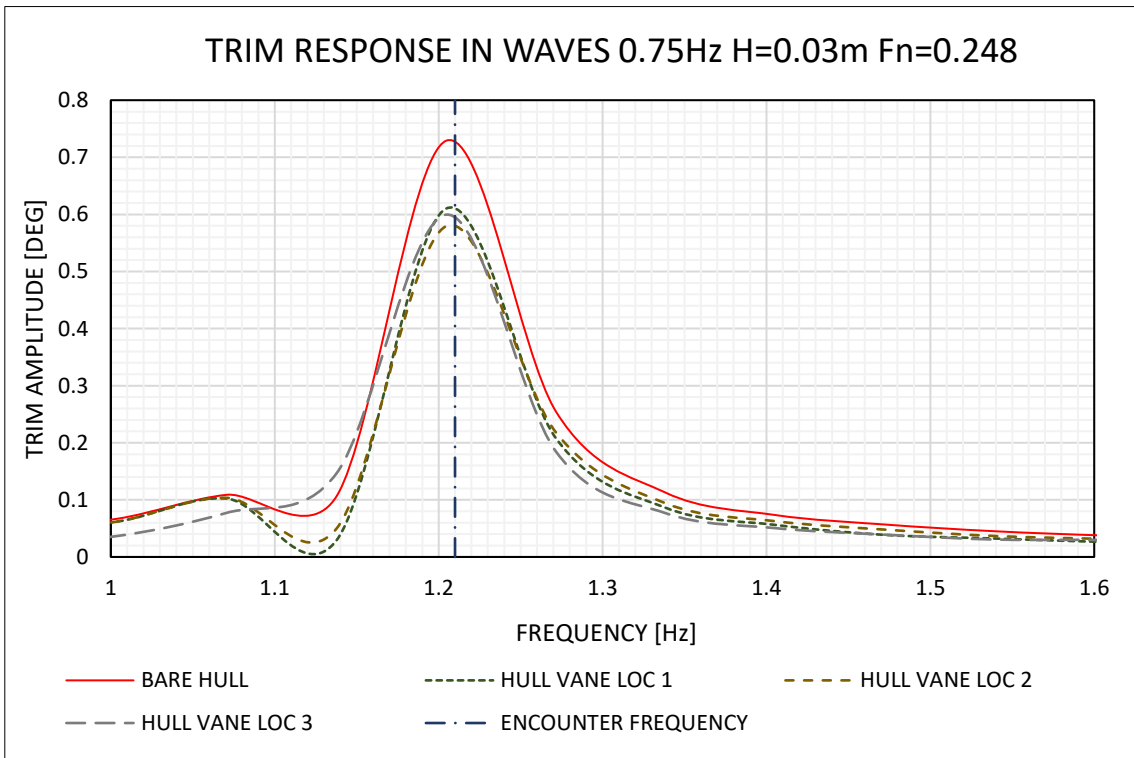


**Fig. 24 Frequency domain trim response in 0.03m wave at Fn=0.248**

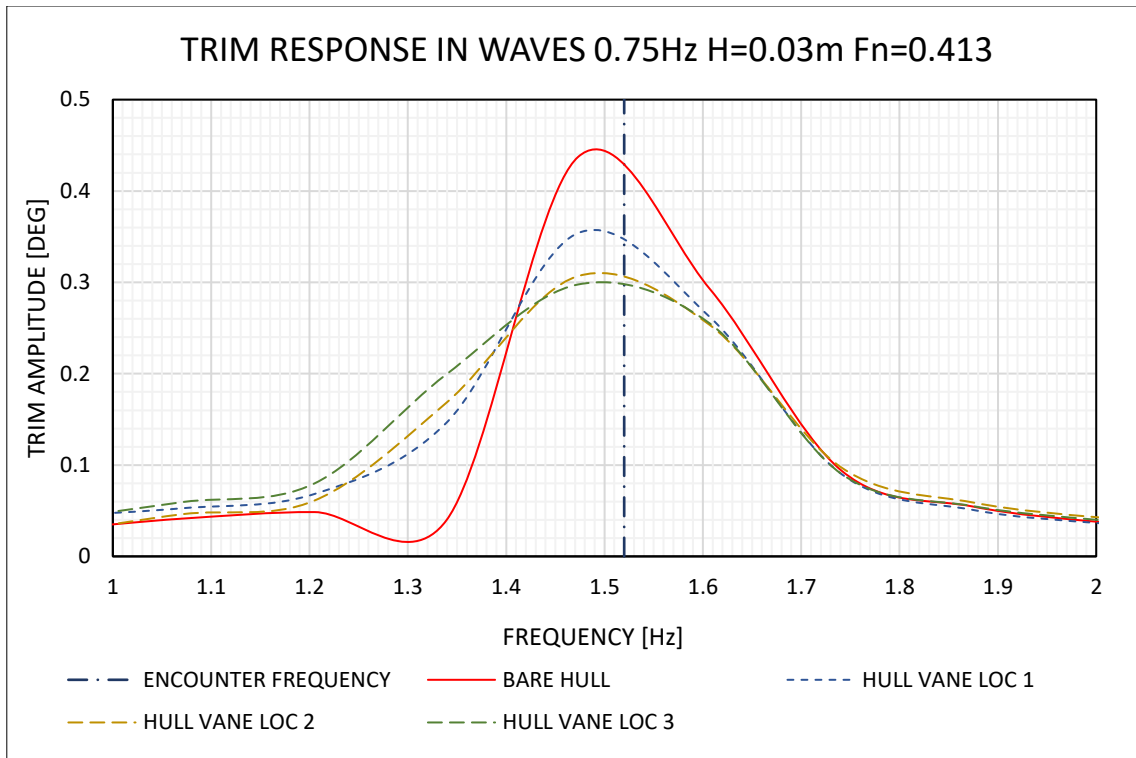


**Fig. 25 Frequency domain trim response in 0.03m wave at Fn=0.413**

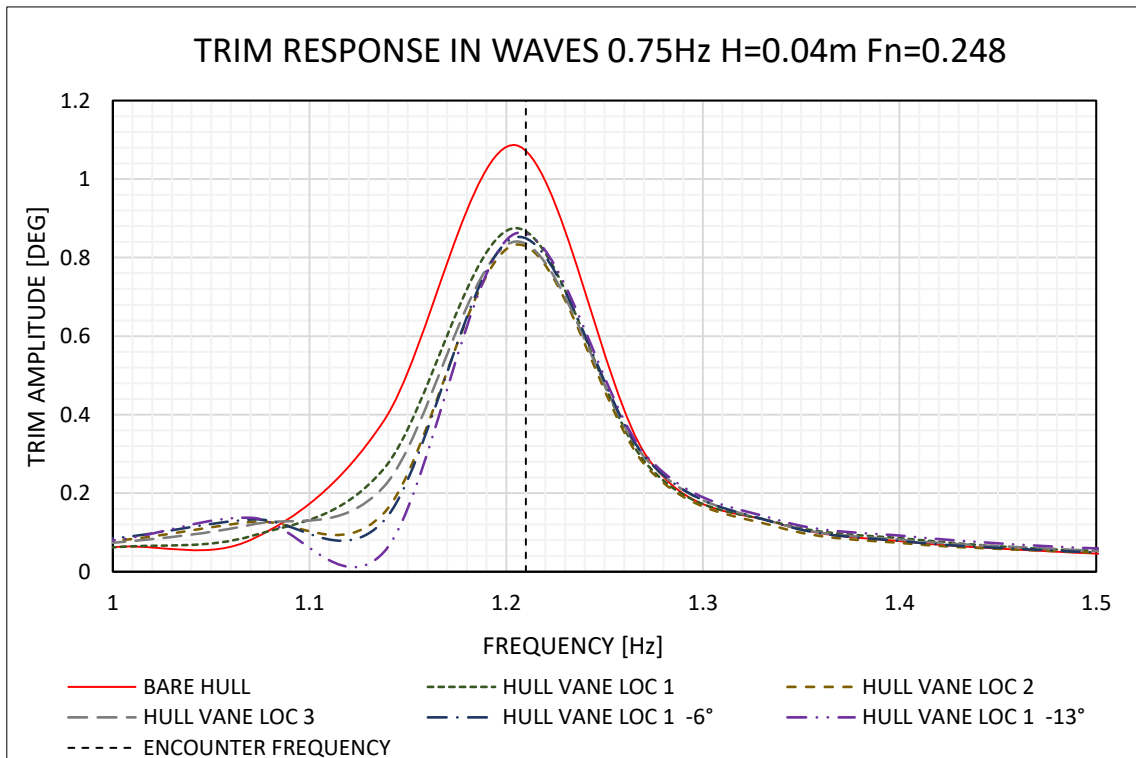


**Fig. 26 Frequency domain trim response in 0.04m wave at Fn=0.248**

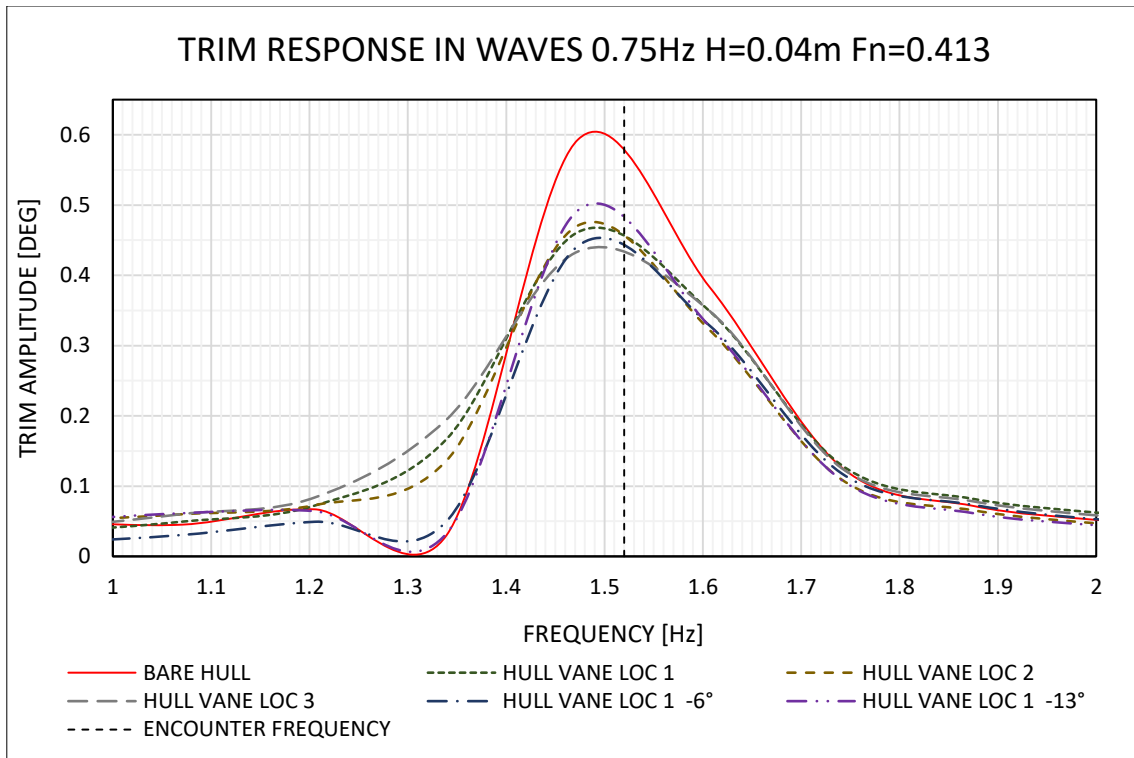


**Fig. 27 Frequency domain trim response in 0.04m wave at Fn=0.413**

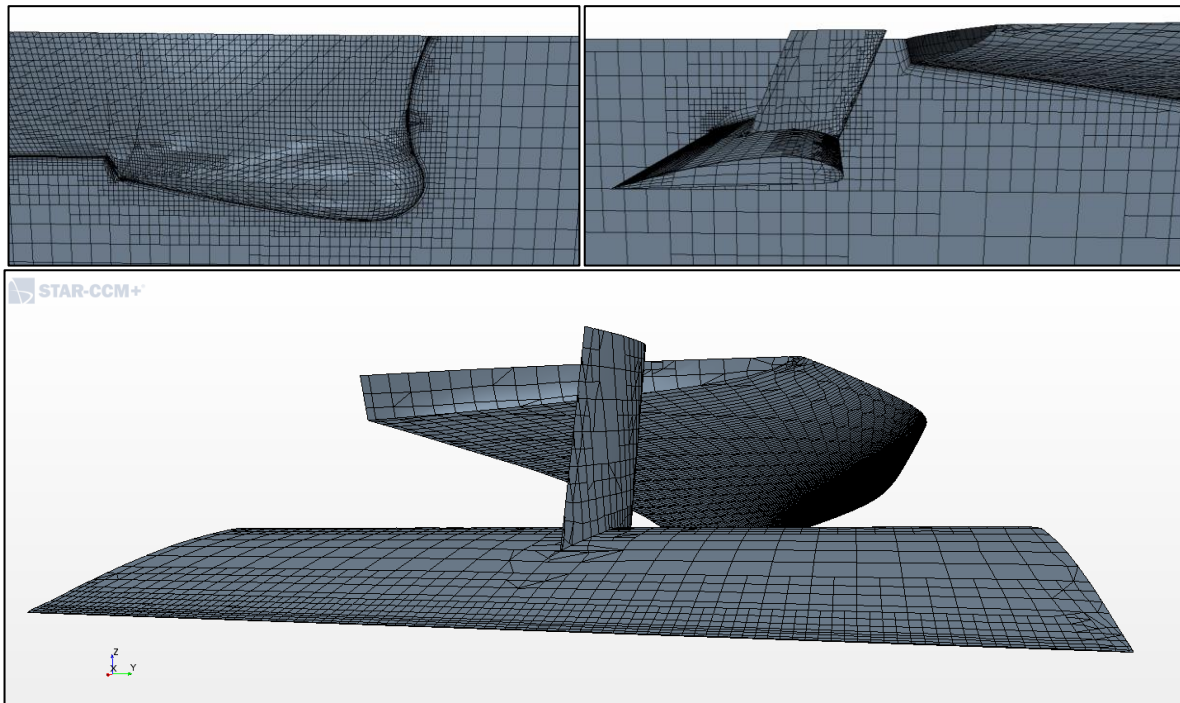


**Fig. 28 Mesh for the CFD analysis**

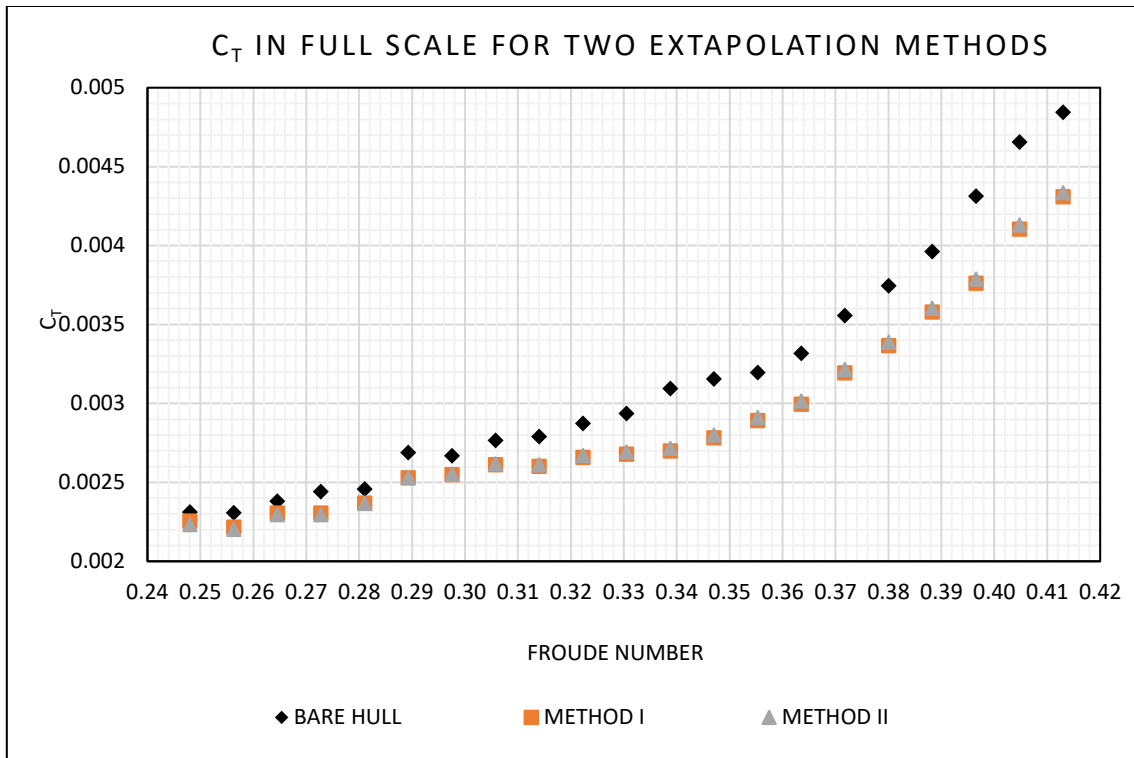


**Fig. 29 Resistance coefficients for Method I and Method II Figure 1**

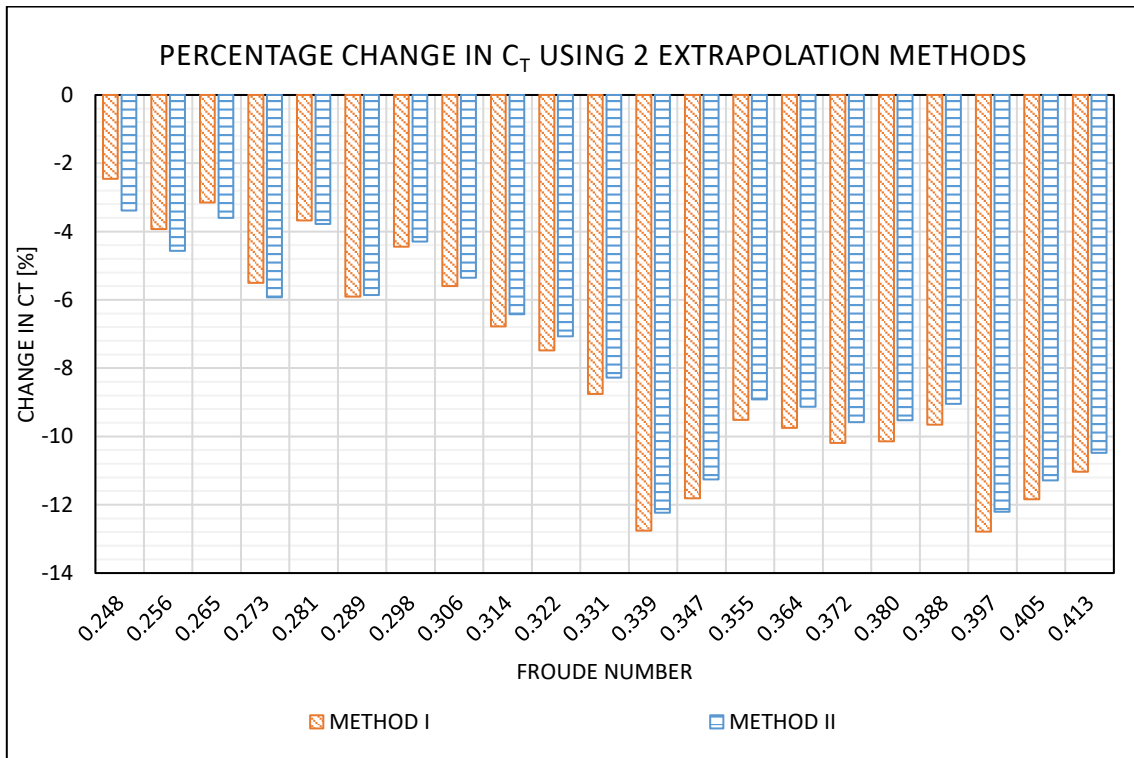


**Fig. 30 Percentage change in full-scale  $C_T$  for two extrapolation methods**

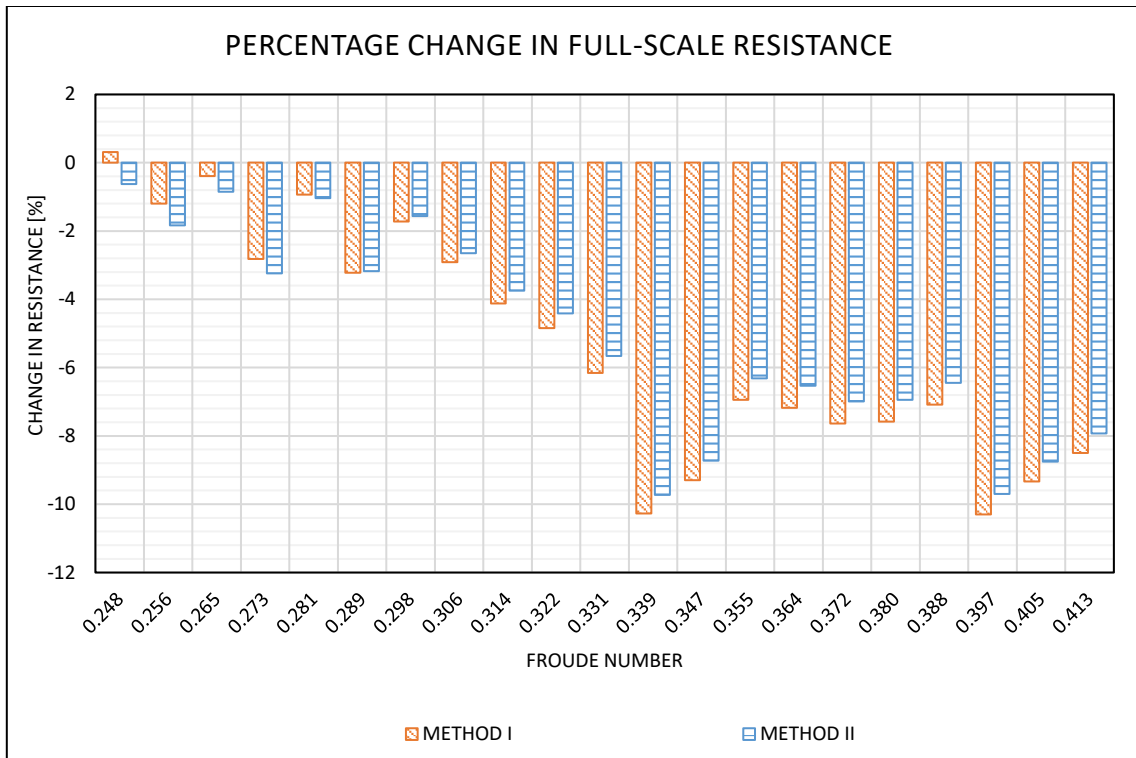


**Fig.31 Percentage change in the full-scale resistance using Method I and Method II**

## Tables

**Table 1 the relationship between the four energy saving devices**

Function	Correct trim	Reduce stern wave	Damp pitch motion	Additional thrust
Interceptor	√		√	
Stern End Bulb		√		
Bow Foil			√	√
Hull Vane	√	√	√	√

**Table 2 Main particulars of full-scale and model-scale hull**

PARAMETERS	UNITS	FULL SCALE	MODEL SCALE
LPP (m)	m	142	2.784
Lwl (m)	m	142.18	2.788
Bwl	m	19.06	0.374
T	m	6.15	0.121
Displacement	m <sup>3</sup>	8424.4	0.066
Wetted Surface	m <sup>2</sup>		1.2668
CB		0.507	0.507
CM		0.821	0.821
LCB (%Lpp)		-0.683	-0.683
U=18 knots	m/s	9.26	1.3
U=30 knots	m/s	15.43	2.16
Fn in 18 knots		0.248	0.248
Fn in 30 knots		0.413	0.413

**Table 3 Hull Vane location detail**

		LOCATION 1	LOCATION 2	LOCATION 3
Angle of Attack	deg	2	2	2
Trailing Edge Draft	mm	40	40	50
Trailing Edge to AP	mm	85	105	85

**Table 4 Test matrix for 180 tests**

MODELS	SPEEDS (KNOTS)	VANE LOCATIONS	AOAS (DEGREE)	WAVE CONDITIONS
BARE HULL	18-30			still water
WITH VANE	18-30	1-3	2	still water
WITH VANE	18-30	1	-30~17	still water

<b>BARE HULL</b>	18, 30			0.02 ~ 0.04m wave
<b>WITH VANE</b>	18, 30	1-3	2	0.02 ~ 0.04m wave
<b>WITH VANE</b>	18, 30	1	-30~17	0.04 m wave